

## Hidden Phase of the Spin-Boson Model

Florian Otterpohl<sup>1,2,\*</sup>, Peter Nalbach<sup>3</sup>, and Michael Thorwart<sup>2,4</sup>

<sup>1</sup>Center for Computational Quantum Physics, Flatiron Institute, New York, New York 10010, USA

<sup>2</sup>I. Institut für Theoretische Physik, Universität Hamburg, Notkestraße 9, 22607 Hamburg, Germany

<sup>3</sup>Fachbereich Wirtschaft und Informationstechnik, Westfälische Hochschule, Münsterstraße 265 46397 Bocholt, Germany

<sup>4</sup>The Hamburg Centre for Ultrafast Imaging, Luruper Chaussee 149, 22761 Hamburg, Germany



(Received 28 February 2022; accepted 7 September 2022; published 16 September 2022)

A quantum two-level system immersed in a sub-Ohmic bath experiences enhanced low-frequency quantum statistical fluctuations which render the nonequilibrium quantum dynamics highly non-Markovian. Upon using the numerically exact time-evolving matrix product operator approach, we investigate the phase diagram of the polarization dynamics. In addition to the known phases of damped coherent oscillatory dynamics and overdamped decay, we identify a new third region in the phase diagram for strong coupling showing an aperiodic behavior. We determine the corresponding phase boundaries. The dynamics of the quantum two-state system herein is not coherent by itself but slaved to the oscillatory bath dynamics.

DOI: [10.1103/PhysRevLett.129.120406](https://doi.org/10.1103/PhysRevLett.129.120406)

**Introduction.**—Dissipative environments are the cause of relaxation and decoherence in quantum systems. Accordingly, understanding and modeling their influence and subsequently tailoring their impact is relevant to many research areas [1,2]. At strong system-bath coupling, dissipative environments may also lead to fully incoherent dynamics or even complete suppression of the dynamics (localization). Generally it is believed that, while prominent environmental modes may well cause coherent oscillations in a quantum system, a broadband reservoir destroys coherence at sufficiently strong coupling [3,4].

Typically, a quantum two-state system interacting with harmonic degrees of freedom (spin-boson model) is studied [1,2]. At low temperatures and weak coupling damped coherent oscillations are observed while at stronger dissipation a classical incoherent decay toward thermal equilibrium is found. For an Ohmic bath with spectrum  $J(\omega) \propto \alpha\omega^s$  and spectral exponent  $s = 1$  the ratio of the damping rate and oscillation frequency is independent of the oscillation frequency. With increasing coupling  $\alpha$  the dynamics turns incoherent and, for even larger coupling, a zero temperature phase transition toward a localized phase is observed [1,2].

While super-Ohmic spectra with  $s > 1$  with more pronounced high-frequency modes do not show incoherent dynamics or a localization transition, reservoirs with more pronounced low-frequency spectra such as sub-Ohmic ones with  $s < 1$  exhibit a localization phase transition [5–7] and are relevant for quantum impurity systems [8,9]. In contrast, the dynamic transition to incoherent behavior is far less studied although this class of reservoirs constitutes the dominant noise source in, for example, nanomechanical oscillator systems [10] and superconducting qubit

architectures (specifically charge noise generated by two-level fluctuators) [11–13]. Although originally believed to always be incoherent [1], it is now well established that for  $1/2 \lesssim s \leq 1$  with increasing coupling the dynamics turns from damped oscillatory to incoherent, and for larger coupling a transition to a localized phase takes place [14–17]. For  $0 \leq s \lesssim 1/2$ , however, Kast and Ankerhold [16] showed that oscillatory dynamics persists for arbitrary coupling strength for an initially polarized bath. Pure dephasing sub-Ohmic reservoirs influence a quantum two-state system in a similar way and result in overdamping only for  $\omega_c \rightarrow \infty$  and  $s \gtrsim 0.1$  [18].

This leaves two important questions: What happens when crossing the supposed phase boundary at  $s \simeq 1/2$  for a fixed but strong coupling, and why can strong sub-Ohmic fluctuations not turn the system dynamics incoherent? We investigate the dynamics for  $1/2 \lesssim s \leq 1$  and increasing strength of the coupling to the environment and observe that it turns from coherent to incoherent for a coupling  $\alpha_D(s)$  which depends on the spectral exponent  $s$ . For even larger couplings we encounter a sharp phase boundary at a coupling  $\alpha_B(s)$  to aperiodic behavior, i.e., the dynamics is not fully incoherent but exhibits a single turnaround. This new phase extends to all  $0 \leq s \leq 1$ . For  $0 \leq s \lesssim 1/2$ , where Ref. [16] reports damped oscillatory dynamics for all couplings, we find with increasing coupling a sharp transition from oscillatory dynamics with various minima and maxima to aperiodic dynamics with a single minimum for an initially unpolarized bath. The frequency related to the minimum is proportional to the reservoir cutoff frequency. Accordingly, this dynamics is not generated by the central quantum system but by the reservoir, and it turns incoherent for  $\omega_c \rightarrow \infty$ . We simulate

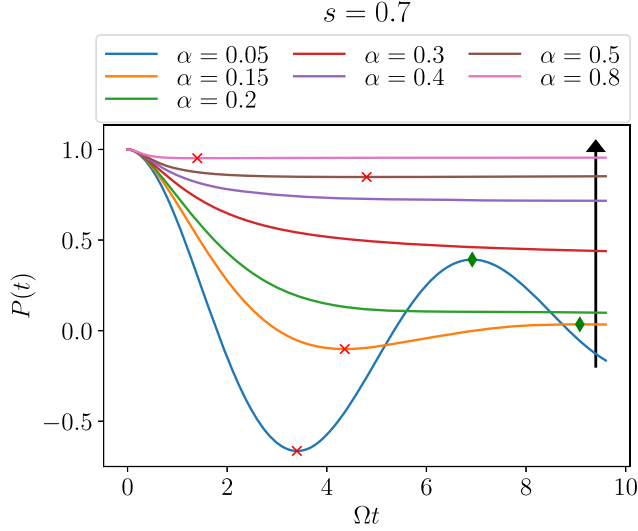


FIG. 1. Polarization  $P(t)$  for  $T = 0$ ,  $s = 0.7$ , and different coupling strengths  $\alpha$ . The arrow intersects the lines in ascending order of coupling strengths. Local minima (maxima) are marked by a red cross (green diamond).

the dynamics in a broad range of parameters in order to map the new phase diagram of the dynamical behavior of the spin-boson model.

*Model.*—We consider the symmetric spin-boson model ( $\hbar = 1$ ,  $k_B = 1$ ) with the Hamiltonian

$$\begin{aligned} \hat{H} &= \hat{H}_S + \hat{H}_B + \hat{H}_{\text{int}} \\ &= \frac{\Omega}{2} \hat{\sigma}_x + \frac{1}{2} \sum_j (\hat{p}_j^2 + \omega_j \hat{x}_j^2) + \frac{\hat{\sigma}_z}{2} \hat{\xi}, \end{aligned} \quad (1)$$

where  $\hat{\xi} = \sum_j c_j \hat{x}_j$ ,  $\Omega$  is the tunneling splitting, and  $\hat{\sigma}_{x/z}$  are the Pauli matrices. The bath consists of harmonic oscillators with momenta  $\hat{p}_j$ , angular frequencies  $\omega_j$ , and positions  $\hat{x}_j$  which are coupled via coupling constants  $c_j$  to the spin. The bath has the spectral density

$$J(\omega) = \sum_j \frac{c_j^2}{2\omega_j} \delta(\omega - \omega_j) = 2\alpha \frac{\omega^s}{\omega_c^{s-1}} e^{-\omega/\omega_c}, \quad (2)$$

with the high-frequency cutoff  $\omega_c = 10\Omega$  (unless specified otherwise) and the coupling strength  $\alpha$ . We focus on the (sub-)Ohmic regime where  $0 \leq s \leq 1$ . We calculate the time-dependent polarization  $P(t) = \langle \sigma_z \rangle(t)$ , using a factorizing initial preparation of the system with  $P(0) = 1$  and the thermal distribution of the initially uncoupled (i.e., unpolarized) bath at zero temperature.

*Method.*—To determine  $P(t)$  we use the numerically exact real-time quadiabatic propagator path integral (QUAPI) [19–24]. Once the bath oscillators have been integrated out, an effective dynamics of the system arises which is nonlocal in time. To treat the highly entangled system-bath dynamics of the sub-Ohmic spin-boson model,

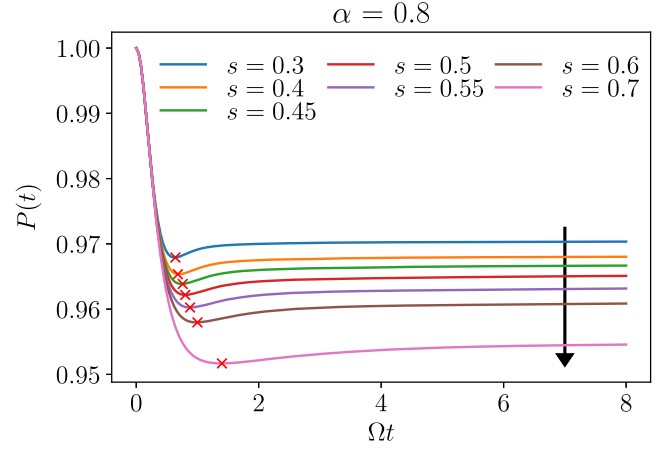


FIG. 2. Polarization  $P(t)$  for  $T = 0$ ,  $\alpha = 0.8$ , and different spectral exponents  $s$ . The arrow intersects the lines in ascending order of spectral exponents. Local minima are marked with a red cross.

we make use of the time-evolving matrix product operator technique [23,24]; see the Supplemental Material [25] for further details. It allows us to avoid the conventional QUAPI memory cutoff as it rewrites the arising discrete path-sum in terms of a numerically highly efficient tensor network.

*Polarization dynamics.*—First, we investigate the dynamics for a fixed  $s = 0.7$  for increasing coupling  $\alpha$ . Figure 1 shows the time-dependent polarization  $P(t)$  for times up to  $\Omega t \lesssim 10$ . For  $\alpha = 0.05$  and  $\alpha = 0.15$ , we observe damped oscillatory or coherent dynamics with a minimum (marked by a red cross in Fig. 1) and a maximum (marked by a green diamond) visible in the studied time frame. But for couplings  $\alpha = 0.2$  and  $\alpha = 0.4$ , we find a monotonic decay highlighting purely incoherent dynamics. Surprisingly, for larger couplings  $\alpha \geq 0.5$  we find again a minimum but no subsequent maximum. We denote this dynamics pseudocoherent in the following.

Next we decrease the spectral exponent  $s$  for a large but fixed system-bath coupling strength  $\alpha = 0.8$  with dynamics in the pseudocoherent phase from  $s = 0.7$  to  $0.3$ . Figure 2 depicts the according time-dependent polarization  $P(t)$ . In all cases we observe pseudocoherent dynamics with a single minimum (marked by a red cross). With decreasing  $s$ , the minimum shifts to earlier times. No qualitative change in the dynamic behavior is found upon decreasing  $s$  below  $s = 1/2$ . For  $s \lesssim 1/2$ , Kast and Ankerhold [16] have shown that no transition to incoherent dynamics occurs irrespective of the coupling strength.

Figure 3 shows the polarization for various coupling strengths for a fixed  $s = 0.3$ . For couplings from  $\alpha = 0.8$  down to  $\alpha = 0.125$ , we observe pseudocoherent dynamics with only one minimum. For  $\alpha = 0.1$  and  $\alpha = 0.05$ , we find coherent dynamics with a minimum and a maximum.

*Phase diagram.*—Next we examine the full parameter space of  $0 \leq s \leq 1$  and  $\alpha$ . We observe sharp transitions

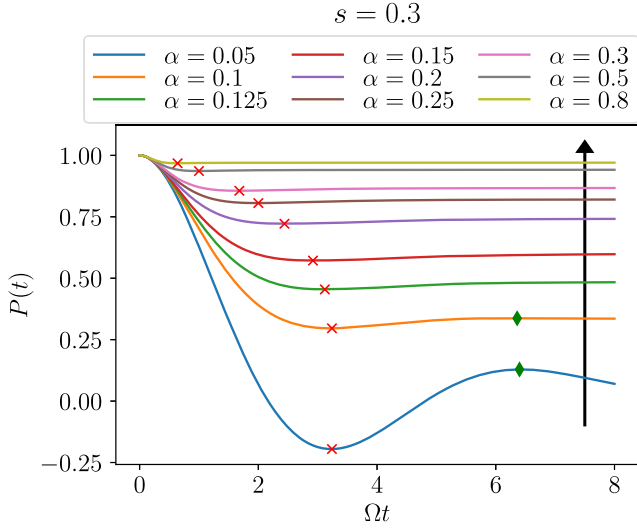


FIG. 3. Polarization  $P(t)$  for  $T = 0$ ,  $s = 0.3$ , and different coupling strengths  $\alpha$ . The arrow intersects the lines in ascending order of coupling strengths. Local minima (maxima) are marked by a red cross (green diamond).

between three dynamical phases: coherent dynamics, i.e., damped oscillatory behavior with minima and maxima; incoherent dynamics, i.e., purely monotonic decay; and pseudocoherent dynamics, i.e., a single minimum and subsequent decay into localization. The observed phase diagram is sketched in Fig. 4. For  $\alpha = 0$ , the time-dependent polarization is  $P(t) = \cos(\Omega t)$  with its first local minimum at  $\Omega t = \pi$ . As the dynamics depends continuously on the parameters  $\alpha$  and  $s$ , we can track this local minimum when increasing the coupling strength. For  $s \gtrsim 0.45$ , we find that this minimum vanishes if the coupling strength is sufficiently increased leading to the transition from coherent to incoherent dynamics at  $\alpha_D(s)$  (depicted as blue crosses in Fig. 4). Our results coincide with the results shown in Fig. 5 of Ref. [17] for  $s > 0.5$ . Increasing the coupling strength further, we enter the pseudocoherent phase at  $\alpha_B(s)$  (depicted by orange diamonds). For  $s \leq 0.45$  we track the first local maximum of the coherent phase, which vanishes in the transition to the pseudocoherent regime (see Fig. 3 for  $s = 0.3$ ). The green circles in Fig. 4 depict the coupling strength  $\alpha_B(s)$  of the respective phase transition from coherent to pseudocoherent dynamics. Note that while maxima in the dynamics of the pseudocoherent phase at very long times, i.e., time-scales not determined by  $\Omega$  or  $\omega_c$  (which we cannot strictly rule out due to finite simulation times), would add to the characteristics of the pseudocoherent phase, they would not change the phase diagram which is determined by sharp transitions between different dynamic behavior at times well within our simulation time window.

*Pseudocoherent phase.*—Next, we investigate the pseudocoherent phase in more detail. Figure 5 shows the quantity  $1 - P(t)$  versus the rescaled time  $\omega_c t$  for various

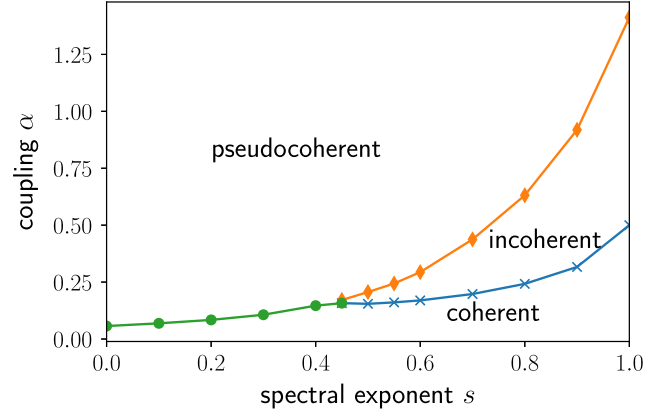


FIG. 4. Phase diagram of the (sub-)Ohmic spin-boson model at  $T = 0$  and  $\omega_c = 10\Omega$ . The symbols represent coupling strengths  $\alpha(s)$  at which a transition occurs and are linearly interpolated for better visibility. Blue cross: the first local minimum vanishes when increasing coupling out of the coherent to the incoherent domain. Orange diamond: a local minimum appears for  $\Omega t < 8$  when increasing coupling strength out of the incoherent domain. Green circle: the first local maximum vanishes when going from the coherent to the pseudocoherent domain.

$\omega_c$  for  $s = 0.3$  and  $\alpha = 0.8$ . (Note that the minima in  $P(t)$  are maxima in this plot). We observe that the maximum in  $1 - P(t)$  [corresponding to a minimum in  $P(t)$ ] for sufficiently large values of  $\omega_c \gtrsim 10\Omega$  occurs at a time  $t_{\min} \simeq \text{const}/\omega_c$ . Hence, the observed oscillatory behavior in this phase is purely bath driven and therefore distinct from coherence, which generally refers to a behavior inherent to the system. This furthermore suggests that for  $\omega_c \rightarrow \infty$  the polarization  $P(t)$  approaches 1 and the minimum is attained at  $t_{\min} \rightarrow 0$ . Thus, only incoherent fully localized behavior emerges, i.e., the observed oscillatory behavior in the pseudocoherent phase is a result of

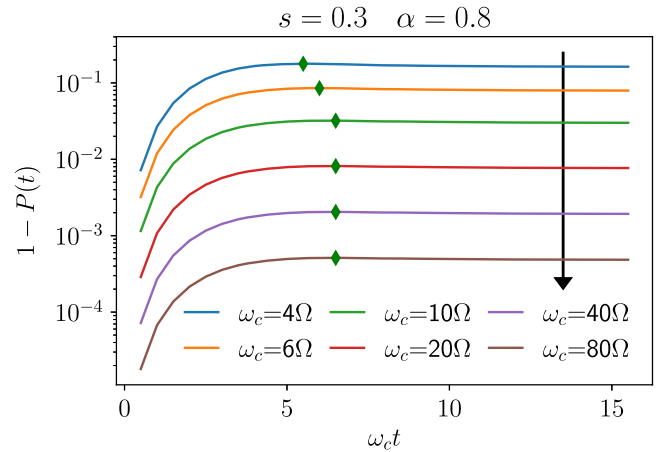


FIG. 5. Polarization  $1 - P(t)$  for  $T = 0$ ,  $\alpha = 0.8$ ,  $s = 0.3$ , and different bath cutoff frequencies  $\omega_c$ . The arrow intersects the lines in ascending order of cutoff frequencies. Local maxima are marked with a green diamond. Note that the  $\omega_c = 10\Omega$  line corresponds to the  $s = 0.3$  line in Fig. 2.

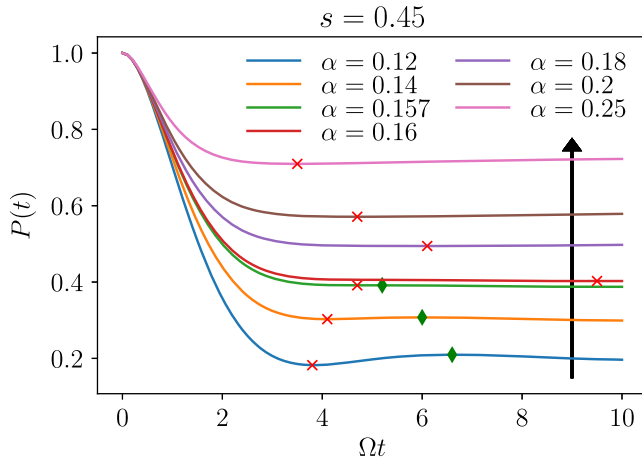


FIG. 6. Polarization  $P(t)$  for  $T = 0$ ,  $s = 0.45$ , and different coupling strengths  $\alpha$ . The arrow intersects the lines in ascending order of coupling strengths. Local minima (maxima) are marked with a red cross (green diamond).

the finite bath reaction time of  $\mathcal{O}(1/\omega_c)$  only after which the system is drawn into localization. Similarly, purely dephasing sub-Ohmic reservoirs with small  $s$  renormalize the oscillation frequency to values larger than its damping rate, with the effect that the renormalized effective frequency vanishes in that regime [18]. Thus, the dynamics never becomes fully overdamped.

Because the oscillation frequency is renormalized in the case of a polarized bath that is initially equilibrated to a spin pointing up, the oscillatory behavior in Ref. [16] also shows maxima in the pseudocoherent phase. Nevertheless, the dynamics in that case is generated by the bath in the same way (for details, see the Supplemental Material [25]).

Increasing  $\omega_c$  also changes the phase separation line  $\alpha_B(s)$ . To determine the phase separation line  $\alpha_B(s)$ , we simulate the polarization dynamics to roughly similar times, i.e.,  $\Omega t \approx 10$  for every  $\omega_c$ . Thus, we are here limited to a fairly small regime of  $\omega_c \leq 50\Omega$  to ensure numerical accuracy. For all studied values of  $\omega_c$  we find that  $\alpha_B(s) > \alpha_c(s)$  with the critical coupling strength  $\alpha_c(s)$  for the thermodynamic  $T = 0$  phase transition to localization. We find that  $\alpha_B(s)$  decreases with increasing  $\omega_c$ .

Our investigation allows us to conclude that for  $\omega_c \rightarrow \infty$  the pseudocoherent phase turns fully incoherent. Thus, for  $s \gtrsim 0.45$  it seems reasonable that  $\alpha_B(s, \omega_c) \rightarrow \alpha_c(s, \omega_c)$  since for couplings smaller than  $\alpha_B(s, \omega_c)$  the dynamics is already incoherent for all  $\omega_c$ . For  $s \lesssim 0.45$  the situation is less clear, and it remains open whether for  $\omega_c \rightarrow \infty$  there is a coupling regime with damped coherent dynamics. We should point out that the limit of infinite  $\omega_c$  is also not clear for  $\alpha_c$ , i.e., the thermodynamic localization transition, except for Ohmic bath spectra where  $\alpha_c(s = 1, \omega_c \rightarrow \infty) = 1$ . For  $0 \leq s \leq 1/2$  a variational approach yields  $\alpha_c(s, \omega_c \rightarrow \infty) \rightarrow 0$  [26].

*Spectral crossover.*—Investigations of the thermodynamic localization phase transition [6], i.e., the according

critical exponents, conclude that  $s = 1/2$  is the border between mean-field behavior for  $s < 1/2$  and non-mean-field for  $s > 1/2$ . We find a crossover  $s_{\text{cross}}$  with a possible incoherent phase for  $s > s_{\text{cross}}$  and no incoherent phase for  $s < s_{\text{cross}}$  at  $s_{\text{cross}} \approx 0.45$  (see Fig. 4), which is consistent with the results of Duan *et al.* [17] that imply  $s_{\text{cross}} \lesssim 0.525$ . Figure 6 shows the polarization for  $T = 0$ ,  $s = 0.45$ , and different coupling strengths  $\alpha$ . For  $\alpha = 0.12$ , we observe coherent dynamics with a minimum and maximum. For increasing couplings, i.e.,  $\alpha = 0.14$  and  $0.157$ , both merge. For  $\alpha = 0.16$ , a new single minimum at latest observed time appears which for further increasing coupling shifts to earlier times. For  $s < 0.45$  (see, for example, Fig. 3), the observed minimum in the pseudocoherent phase emerges from the first minimum in the coherent phase. It remains an open question how this crossover  $s$  depends on  $\omega_c$  and how far it is connected to the crossover from mean-field to non-mean-field type thermodynamics phase behavior.

*Conclusion.*—By means of numerically exact real-time path integral simulations, we have studied the nonequilibrium dynamics of the (sub-)Ohmic spin-boson model. Analyzing the polarization dynamics, we find for all spectral exponents  $0 \leq s \leq 1$  at strong coupling a pseudocoherent phase whose hallmark is a single oscillatory minimum. In particular for  $0.45 \leq s \leq 1$ , we observe this new dynamical phase at strong coupling beside the well-known coherent dynamics at weak coupling and incoherent dynamics at intermediate coupling. Oscillatory dynamics for  $0 \leq s \leq 1/2$  for all couplings has been observed by Kast and Ankerhold [16] before. We show that for these  $s$  there is nevertheless a transition from coherent (many minima and maxima in the polarization dynamics) to pseudocoherent dynamics (with a single minimum). The frequency related to the oscillatory minimum in the pseudocoherent phase is proportional to the bath cutoff frequency. Accordingly, this dynamics is not generated by the two-level system but by the reservoir, and it turns incoherent for  $\omega_c \rightarrow \infty$ . We map the full dynamical phase diagram with now three distinct phases.

F. O. is grateful for the kind hospitality at the Flatiron Institute where parts of this work have been carried out. The Flatiron Institute is a division of the Simons Foundation. M. T. acknowledges support by the Cluster of Excellence ‘‘CUI: Advanced Imaging of Matter’’ of the Deutsche Forschungsgemeinschaft (DFG)—EXC 2056—project ID 390715994.

\*florian.otterpohl@physik.uni-hamburg.de

- [1] A. J. Leggett, S. Chakravarty, A. T. Dorsey, M. P. A. Fisher, A. Garg, and W. Zwerger, Dynamics of the dissipative two-state system, *Rev. Mod. Phys.* **59**, 1 (1987).
- [2] U. Weiss, *Quantum Dissipative Systems*, 4th ed. (World Scientific, Singapore, 2012).

- [3] J. Iles-Smith, N. Lambert, and A. Nazir, Environmental dynamics, correlations, and the emergence of noncanonical equilibrium states in open quantum systems, *Phys. Rev. A* **90**, 032114 (2014).
- [4] H. Maguire, J. Iles-Smith, and A. Nazir, Environmental Nonadditivity and Franck-Condon Physics in Nonequilibrium Quantum Systems, *Phys. Rev. Lett.* **123**, 093601 (2019).
- [5] F.B. Anders, R. Bulla, and M. Vojta, Equilibrium and Nonequilibrium Dynamics of the Sub-Ohmic Spin-Boson Model, *Phys. Rev. Lett.* **98**, 210402 (2007).
- [6] A. Winter, H. Rieger, M. Vojta, and R. Bulla, Quantum Phase Transition in the Sub-Ohmic Spin-Boson Model: Quantum Monte Carlo Study with a Continuous Imaginary Time Cluster Algorithm, *Phys. Rev. Lett.* **102**, 030601 (2009).
- [7] A. Alvermann and H. Fehske, Sparse Polynomial Space Approach to Dissipative Quantum Systems: Application to the Sub-Ohmic Spin-Boson Model, *Phys. Rev. Lett.* **102**, 150601 (2009).
- [8] Q. Si, S. Rabello, K. Ingersent, and J.L. Smith, Locally critical quantum phase transitions in strongly correlated metals, *Nature (London)* **413**, 804 (2001).
- [9] P. Gegenwart, T. Westerkamp, C. Krellner, Y. Tokiwa, S. Paschen, C. Geibel, F. Steglich, E. Abrahams, and Q. Si, Multiple energy scales at a quantum critical point, *Science* **315**, 969 (2007).
- [10] S. Gröblacher, A. Trubarov, N. Prigge, G.D. Cole, M. Aspelmeyer, and J. Eisert, Observation of non-Markovian micromechanical Brownian motion, *Nat. Commun.* **6**, 7606 (2015).
- [11] O. Astafiev, Y. A. Pashkin, Y. Nakamura, T. Yamamoto, and J. S. Tsai, Quantum Noise in the Josephson Charge Qubit, *Phys. Rev. Lett.* **93**, 267007 (2004).
- [12] A. Shnirman, G. Schön, I. Martin, and Y. Makhlin, Low- and High-Frequency Noise from Coherent Two-Level Systems, *Phys. Rev. Lett.* **94**, 127002 (2005).
- [13] X. You, A. A. Clerk, and J. Koch, Positive- and negative-frequency noise from an ensemble of two-level fluctuators, *Phys. Rev. Research* **3**, 013045 (2021).
- [14] A. Chin and M. Turlakov, Coherent-incoherent transition in the sub-Ohmic spin-boson model, *Phys. Rev. B* **73**, 075311 (2006).
- [15] P. Nalbach and M. Thorwart, Ultraslow quantum dynamics in a sub-Ohmic heat bath, *Phys. Rev. B* **81**, 054308 (2010).
- [16] D. Kast and J. Ankerhold, Persistence of Coherent Quantum Dynamics at Strong Dissipation, *Phys. Rev. Lett.* **110**, 010402 (2013).
- [17] C. Duan, Z. Tang, J. Cao, and J. Wu, Zero-temperature localization in a sub-Ohmic spin-boson model investigated by an extended hierarchy equation of motion, *Phys. Rev. B* **95**, 214308 (2017).
- [18] P. Nalbach and M. Thorwart, Crossover from coherent to incoherent quantum dynamics due to sub-Ohmic dephasing, *Phys. Rev. B* **87**, 014116 (2013).
- [19] N. Makri, Numerical path integral techniques for long time dynamics of quantum dissipative systems, *J. Math. Phys. (N.Y.)* **36**, 2430 (1995).
- [20] N. Makri and D. E. Makarov, Tensor propagator for iterative quantum time evolution of reduced density matrices. I. Theory, *J. Chem. Phys.* **102**, 4600 (1995).
- [21] N. Makri and D. E. Makarov, Tensor propagator for iterative quantum time evolution of reduced density matrices. II. Numerical methodology, *J. Chem. Phys.* **102**, 4611 (1995).
- [22] N. Makri, Small matrix path integral for system-bath dynamics, *J. Chem. Theory Comput.* **16**, 4038 (2020).
- [23] A. Strathearn, P. Kirton, D. Kilda, J. Keeling, and B. W. Lovett, Efficient non-Markovian quantum dynamics using time-evolving matrix product operators, *Nat. Commun.* **9**, 3322 (2018).
- [24] A. Strathearn, *Modelling Non-Markovian Quantum Systems Using Tensor Networks*, Springer Theses (Springer International Publishing, Cham, 2020).
- [25] See Supplemental Material at <http://link.aps.org/supplemental/10.1103/PhysRevLett.129.120406> for a summary of the time-evolving matrix product operator method, details on the numerical convergence, and additional results for polarized initial conditions of the bath.
- [26] A.W. Chin, J. Prior, S.F. Huelga, and M.B. Plenio, Generalized Polaron Ansatz for the Ground State of the Sub-Ohmic Spin-Boson Model: An Analytic Theory of the Localization Transition, *Phys. Rev. Lett.* **107**, 160601 (2011).